

Preparation and Characterization of Electromagnetic Interference Shielding Polyimide Foam

Xiao-Yan Liu, Mao-Sheng Zhan, Kai Wang

School of Material Science and Engineering, Beijing University of Aeronautics and Astronautics, Beijing 100191, China

Correspondence to: M.-S. Zhan (E-mail: zhanms@buaa.edu.cn)

ABSTRACT: This article focused on the preparation and characterization of ultralight and high-temperature resistant polyimide foam (PIF) for electromagnetic interference shielding. PIF was first prepared based on a one-pot process by the primary reactions of derivatives of pyromellitic dianhydride and polyaryl polymethylene isocyanate. Then, PIFs with silver (0) coating were then prepared by spraying silver (0) on the surfaces of PIF through physical spraying method. The surface density of silver coating was 0.18 kg/m^2 , and the densities of silver-coated PIFs were less than 23 kg/m^3 . The scanning electron microscopy coupled with an energy-dispersive X-ray spectrometer (EDX) measurement were carried out to investigate the morphological and chemical properties of uncoated and coated PIFs. For coated PIFs, the EDX spectrums indicated increasing higher silver proportions from interior to exterior surface, together with increasing higher carbon proportions from exterior surface to interior. Thermogravimetry/Fourier transform infrared instrument that combined thermogravimetric analysis with pyrolysis product analysis by Fourier transform infrared spectroscopy were applied to investigate the thermal stability and pyrolysis products of uncoated and coated PIFs. The results indicated that the thermal properties of silver-coated PIFs were improved obviously with the 5% weight loss temperature higher than 400°C and the residual weight retentions at $800^\circ\text{C} \sim 80\%$. In the frequency range 200–7000 MHz, the EMI shielding efficiency with one surface and two surfaces coated with silver were in the range of 36.4–60.7 dB and 61.6–95.6 dB, respectively. © 2012 Wiley Periodicals, Inc. *J. Appl. Polym. Sci.* 000: 000–000, 2012

KEYWORDS: polyimide foam; ultralight; high temperature resistance; electromagnetic interference shielding

Received 11 March 2012; accepted 29 April 2012; published online

DOI: 10.1002/app.37996

INTRODUCTION

Electromagnetic interference (EMI) has become a more and more serious problem with extensive practical applications of sensitive electronic devices and densely packed systems. Hence, in recent years, considerable attentions have been devoted to the development of effective EMI shielding materials.^{1–4} Polymer with carbon nanotubes (CNTs) or fibers are effective EMI shielding materials.^{5,6} Compared with conventional metal-based and polymer resin EMI shielding materials,⁷ electrically conductive polymer foam composites have excellent advantages such as light weight, resistance to corrosion, good processability, and tunable conductivity. Light weight is important and favorable to the practical EMI shielding application in areas of aircraft, spacecraft, and automobiles. Therefore, electrically conductive polymer foams have gained popularity for EMI shielding applications.

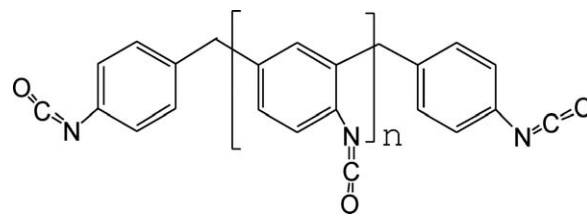
Yang et al.^{8,9} developed novel carbon-nanotubes- and carbon-nanofibers (CNFs)-filled polystyrene (PS) conductive foam composite for EMI shielding. The EMI shielding efficiency of

PS nanocomposite foam with 7 wt % CNTs in the frequency range 8.2–12.4 GHz was nearly 20 dB, much higher than that (~ 9 dB) of PS nanocomposite foam with 7 wt % CNFs. However, these nanocomposite foams were heterogeneous with relatively high densities. Afterwards, they added a gas-producing foaming agent 2,2'-azoisobutyronitrile into the mixture solution of dispersed CNFs and PS resin matrix. The EMI shielding efficiency of PS nanocomposite foam with 15 wt % CNFs was ~ 19 dB in the X-band frequency region. Zhang et al.¹⁰ reported on the preparation of functional polymethylmethacrylate (PMMA)/graphene nanocomposite microcellular by blending of PMMA with graphene sheets for EMI shielding applications. The graphene-PMMA foam with a low graphene loading of 5 wt % exhibited not only a high conductivity ($\sim 3.11 \text{ S/m}$) but also a good EMI shielding efficiency of 13–19 dB in the frequency range 8.0–12.0 GHz. The question is that the foam density was quite high (790 kg/m^3). Thomassin et al.¹¹ reported an EMI shielding efficiency as high as 60 to 80 dB in polycaprolactone nanofoam filled with multiwalled carbon nanotubes at a very low wt % (~ 2 wt %). The main shielding mechanism of

Table I. The Properties of Some Filled Foam Composites^{8–11}

The additives and matrix	Weight ratio (%)	Density (kg·m ⁻³)	Frequency (GHz)	EMI SE/dB
CNT in PS foam	1	~ 560	8.2–12.4	5.73
	3	~ 560		10.30
	7	~ 560		18.66
CNF in PS foam	1	~ 560		0.73
	3	~ 560		3.09
	7	~ 560		8.53
Graphene in PMMA nanofoam	1.7	650	8–12	4–10
	2.2	610		8–12
	5.0	790		13–19
Multiwalled carbon nanotubess in polycaprolactone nanofoam	0.5	230	26–40	10–15
	1	255		25–40
	2	310		60–80

absorption rather than reflectivity was proposed in their paper. Recently, Xu et al.¹² developed CNTs-filled polyurethane conductive foam for light weight EMI shielding composite. The obtained foam with density being 50 kg/m³ achieved a conductivity of nearly 4.3×10^{-5} S/m. Nevertheless, the EMI shielding properties of this material were not investigated. The properties of some filled foam composites were summarized in Table I.

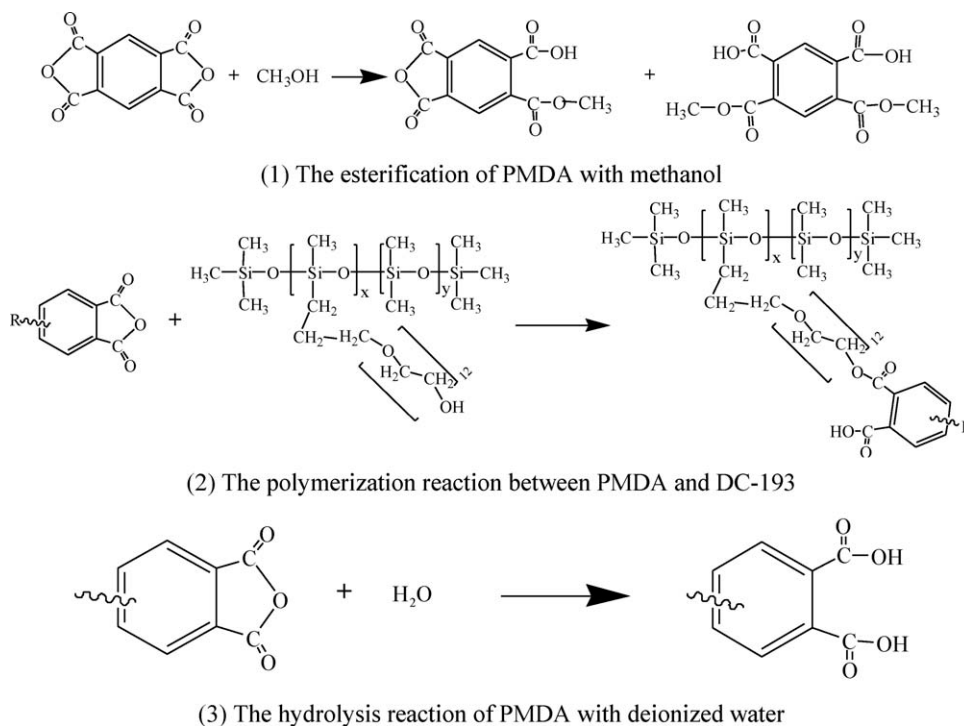
**Scheme 1.** The chemical formula of PAPI.

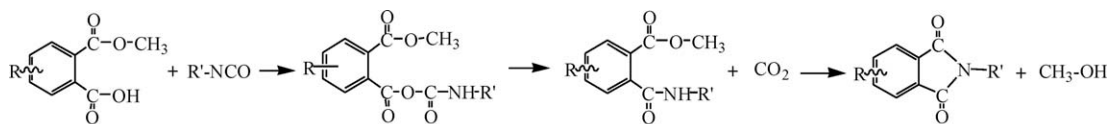
The polymer composite foams in the above mentioned studies exhibited high EMI shielding efficiency, but none of them have solved these problems such as high density and nonuniform structure. For light weight is so important that we should reduce the density of these polymer composite foams. In addition, silver possesses excellent electrical conductivity, and it may also improve the thermal stability and mechanical properties. Therefore, the preparation and characterization of ultralight and high-temperature resistant EMI shielding polyimide foams with silver coatings are presented in this article. It is of interest to note that the EMI shielding efficiency was measured in the frequency range 0.1–7000 MHz. Superior EMI shielding efficiency and improved thermal stability of the silver-coated polyimide foams are expected to be obtained in this article.

EXPERIMENTAL

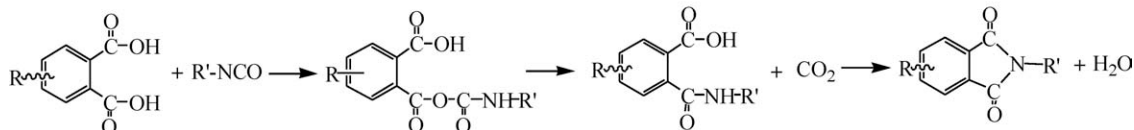
Materials

1,2,4,5-Pyromellitic dianhydride (PMDA) was purchased from Liyang Qingfeng Fine Chemical Plant, China and was dried in a vacuum oven for 8–10 h before use. *N,N*-dimethyl formamide (DMF), methanol, deionized water, triethanolamine, and

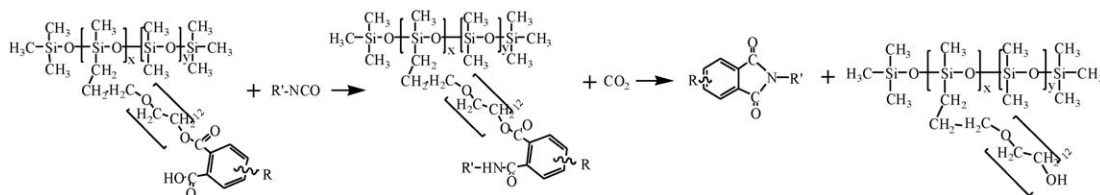
**Scheme 2.** The reactions occurred during the preparation of the first solution.



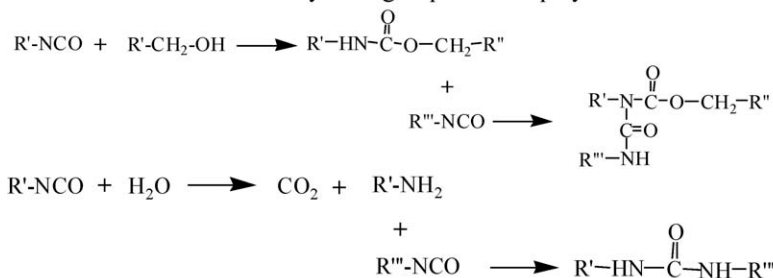
(1) The condensation reaction between isocyanate groups and esterification products



(2) The condensation reaction between isocyanate groups and hydrolyzate



(3) The condensation reaction between isocyanate groups and the polymerisate of PMDA with DC-193



(4) The reactions between isocyanate groups and hydroxyl-containing compounds. Urethane, allophanate and polyurea were generated via these reactions

Scheme 3. The reactions occurred during the foaming process and imidization.

dibutyltin dilaurate were all supplied by Beijing Finechem. Triethanolamine and dibutyltin dilaurate were used as the catalysts. DC-193 (PEG-12 Dimethicone) was acquired from Foshan Daoning Chemical Co., Ltd., China, and it was the surfactant. Polyaryl polymethylene isocyanate (PAPI), a mixture of diphenylmethane diisocyanate and polyfunctional isocyanates, was obtained from Yantai Wanhua Polyurethanes Co., Ltd., China. It is a dark brown liquid with isocyanate content of 30.2–32.0 wt % and viscosity of 150–250 mPa·s at 25°C. The chemical formula of PAPI is shown in Scheme 1.

Preparation of Pure and Silver-Coated Polyimide Foams

Polyimide foam can be prepared according to our previous technique.¹³ First, PMDA was accurately weighed and dissolved in DMF at 55–60°C. The solution was held at temperature and stirred until PMDA was completely dissolved. Then, methanol, DC-193, catalysts, and deionized water were added to the DMF solution and stirred for about 1 h to obtain a first solution. The first solution was cooled to 30°C. The apparent viscosity of the first solution at 30°C was 605 mPa·s. The chemical reactions

and their products which might occur in the first solution are the followings (Scheme 2).

A 50 g sample of the first solution was weighed, and PAPI (~ 25 g) as the second solution was added to the first solution sample. The combined first solution and PAPI was vigorously stirred with a high speed mixer (about 2000 rpm) for ~ 5–15 s. Then, it was immediately transferred to an open mould where it was allowed to rise. Once the foam was no longer tacky, it was placed in a vacuum oven at 250°C to postcure for 3 h to complete the imidization reaction. The obtained polyimide foam with density of 8.3 kg/m³ was expressed as PIF-0. The chemical reactions and their products which might occur during the foaming and postcure are as shown below (Scheme 3).

Two polyimide foam samples were picked out to spray silver (0) on their surfaces by physical spraying method using a K-3 spray gun at room temperature. The nozzle diameter was 0.5 mm and the spray pressure was 0.6 MPa. Polyimide foam is a cellular material; its porous structure cause intimate contact between the silver particles with the rough or uneven foam surfaces

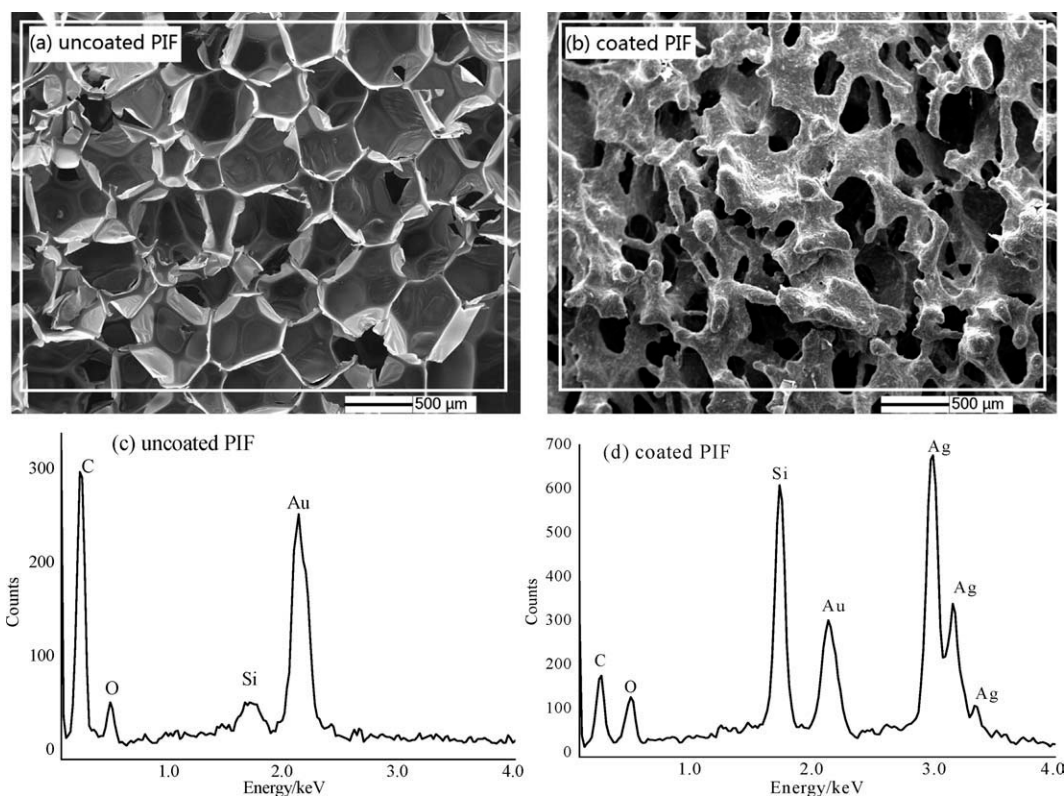


Figure 1. (a) SEM image of uncoated PIF surface, (b) SEM image of silver-coated PIF surface, (c) EDX spectrum of uncoated PIF, and (d) EDX spectrum of silver-coated PIF.

through physical adsorption. Polyimide foam with one surface coated with silver was presented as PIF-1, and the other one with both upper surface and lower surface coated with silver was expressed as PIF-2. The densities of PIF-1 and PIF-2 were 15.6 kg/m^3 and 22.2 kg/m^3 , respectively, and the surface density of the silver coating was 0.18 kg/m^2 .

Characterizations

The apparent viscosity of the first solution was measured by a NDJ-1 rotation viscometer. The cell morphologies of uncoated and coated PIFs were observed using a scanning electron microscopy (SEM, Cam Scan 3400) and a GuiGuang GL-99T stereomicroscope. The chemical compositions were analyzed via EDX spectroscopy (Oxford, INCA Energy). The EMI shielding efficiency of the samples was measured at 20°C in the frequency range 0.1–7000 MHz by a CT-1 flanged coaxial transmission line measuring system, with an E8251A microwave signal source and a E4440A spectrum analyzer. The samples were cut to rectangle plates with dimension of $140 \times 140 \text{ mm}^2$ to fit the waveguide sample holder. Thermogravimetry/Fourier transform infrared (TG-FTIR) instrument that combined thermogravimetric analysis with pyrolysis product analysis by FTIR spectroscopy. The TG-FTIR coupling studies were ramped from 25 to 800°C at $10^\circ\text{C}/\text{min}$ in air. TG analysis was performed with NETZSCH STA TGA-409C, and FTIR spectroscopy was performed with Nicolet Nexus-670. Compressive strengths of the samples were measured on a 5000 kg SANS test stand according to ISO 844: 2004.

RESULTS AND DISCUSSION

Morphological Observations of Uncoated and Silver-Coated PIFs

Identification and characterization of the cross section of uncoated and coated PIFs were performed with a high-resolution SEM coupled with an EDX. Samples placed on the SEM device were coated with a gold-layer to avoid charging of the organic structures under observation and increase the electric conductivity. The cell structures of uncoated and coated PIFs are shown in Figure 1(a) and (b), respectively. As shown in Figure 1(a), the cells are clearly observed and are almost hexagonal with cell membranes and cell struts intact, which is a typical foam structure. The cellular diameter distribution statistics of uncoated PIF (PIF-0) is given in Figure 2. The cell sizes of PIF-0 range from 363 to $681 \mu\text{m}$, which means a very uniform cellular structure. The formation of uniform structure is attributed to the use of foaming agent and its high dispersion with high stirring rate. From Figure 1(a) we can also observe that PIF-0 generally consists of a minimum of two phases, the solid polyimide matrix phase and the gaseous phase.

The SEM image provides visual evidence on the nature of the dispersed silver on the polyimide foam surfaces, shown in Figure 1(b). The surface was completely coated with silver. It can also be seen that the cell membranes are almost broken by the high-speed spraying silver particle, as well as some cell arrises. It is worth noting that the irregular open pores and the cell arrises coated with silver layer may establish electrical conduction pathways throughout the whole surface layer and, therefore,

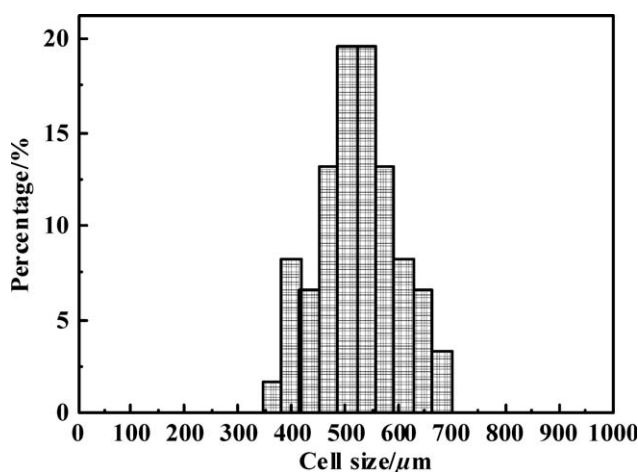


Figure 2. The cellular diameters distribution statistics of PIF-0.

play an important role in determining the EMI shielding efficiency. Besides, coated PIFs are composed of two solid phases, the solid polyimide resin matrix and the silver coating, and the gaseous phase.

EDX was used to identify and characterize the chemical elements found on the polyimide foam surfaces. The element mapping was used to record the two-dimensional elemental composition, which can make us image the distribution of elements like carbon (C), oxygen (O), and silver (Ag). Figure 1(c) and (d) show the EDX spectrums of uncoated and coated polyimide foam surfaces, respectively. The elements and their weight percent are summarized in Table II. As indicated in Figure 1(c), the EDX analysis of uncoated PIF shows that it mainly contained carbon (C), oxygen (O), silicon (Si), and gold (Au), and no evidence suggesting the existence of silver (Ag). The present of silicon (Si) is due to the applied surfactant, DC-193. On the contrary, the EDX analysis of silver-coated PIFs indicates that they contained mostly silver (Ag), together with small amount of other elements such as silicon (Si), carbon (C), and oxygen (O). The appearance of strong peaks at about 3 keV in Figure 1(d) is owing to the fact that the polyimide foam surfaces were entirely coated with silver. The presence of silicon (Si), carbon (C), and oxygen (O) show that the electron probe also detects the substances underneath the depositional silver.

Representative SEM image of the profile of silver-coated PIF structure is shown in Figure 3(a). It can be seen that the silver is mainly dispersed on the surface layer. Typical EDX spectrums of the profile of silver-coated PIFs, recorded with the same characteristics, are shown in Figure 3(b–d). The weight percent of elements in three different regions (Part I, Part II, and Part III) are displayed in Table II. Part I is the region about 0.3 mm from the outside surface. Part II and Part III are the regions about 1.0 mm and 1.7 mm from the outside surface, respectively. It is obvious that the region of Part I is mainly composed of Ag (59.86%), along with small amount of Si (27.91%), C (6.80%), and O (5.43%). The distribution and weight percent of elements in Part III are similar to those in uncoated polyimide foam surface, which is shown in Figure 1(c). It is important to observe that Part I, Part II, and Part III are characterized

by increasing higher silver proportions from interior to exterior surface, together with increasing higher carbon proportions from exterior surface to interior.

EMI Shielding Efficiency of Uncoated and Silver-Coated PIFs

EMI shielding efficiency of uncoated and silver-coated PIFs were determined in the frequency range 0.1 to 7000 MHz. It is known that EMI shielding efficiency is the sum of the reflection from the material surface (SE_R), the absorption of electromagnetic energy (SE_A), and the multiple internal reflections (SE_M) of electromagnetic radiation. Figure 4 shows the variation of EMI shielding efficiency of PIF-0, PIF-1, and PIF-2 in the frequency range 0.1–7000 MHz. The results show that the SE_{total} values of PIF-1 and PIF-2 are almost dependent of frequency in the measured region. In addition, we can also see that the uncoated PIF exhibits hardly any EMI SE_{total} because of its insulating character. After being coated with silver, the SE_{total} values of PIF are enhanced substantially. It is evident that the main contribution to the EMI shielding efficiency comes from the addition of silver.

The electromagnetic waves are absorbed and attenuated by conductive dissipation in PIFs, whereas reflection is the major contribution to the EMI shielding efficiency. As reflection and multiple internal reflections generally increase with increasing silver content, it is reasonable to expect that the SE_{total} values of PIF-2 are higher than those of PIF-1. As illustrated in Figure 4, in the frequency range 0.1–10 MHz, the EMI shielding efficiency of PIF-1 is very close to that of PIF-2. In the frequency range 30–7000 MHz, the SE_{total} values of PIF-2 are obviously higher than that of PIF-1. The results can be explained in the following way. When normal incidence plane electromagnetic waves penetrate the foam sample, most of them were reflected by the conductive silver layer. Parts of the unreflected waves should be at first attenuated by the conductive silver particles attached to the uneven foam surface. When the remaining waves propagate to another surface, they can be reflected again by the silver layer in PIF-2. However, the remaining waves cannot be reflected in PIF-1. In addition, the EMI shielding efficiency of foam materials may be also affected by thickness, density, specific surface area, and other factors. PIF-2 owns higher density and higher percentage of silver/polyimide interfacial area than PIF-1 with the same thickness. There is, in theory, the absorption, reflection, and attenuation of electromagnetic waves in PIF-2 will be stronger than in PIF-1. In fact, PIF-2 owns the higher EMI shielding efficiency than PIF-1, especially at high frequencies.

Table II. The Properties of Uncoated and Silver-Coated PIFs

Foam surface	Weight percent of elements on foam surfaces (%)				
	C	O	Si	Ag	
PIF-0	73.39	25.01	1.60	0	
PIF-1(PIF-2)	6.02	21.36	11.56	61.06	
PIF-1(PIF-2)	Part I	6.80	5.43	27.91	59.86
	Part II	31.72	9.07	22.79	36.42
	Part III	54.42	9.73	23.63	12.22

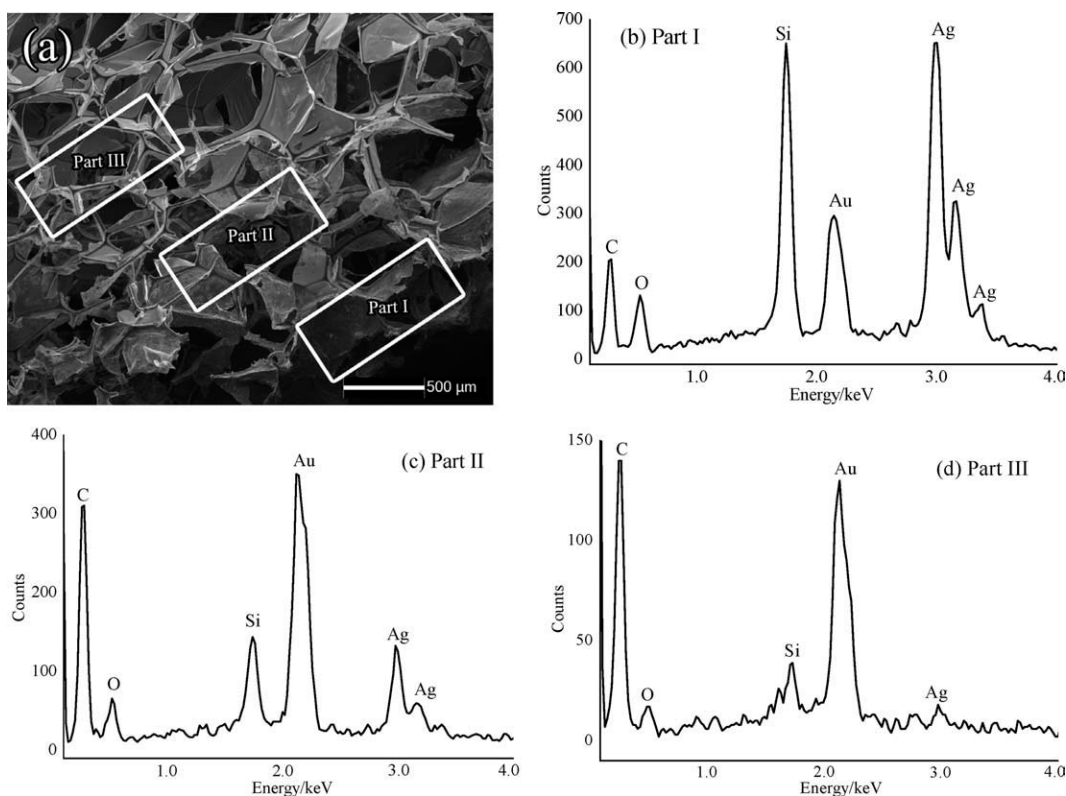


Figure 3. (a) SEM image of the profile of coated PIF, (b) EDX spectrum of coated PIF in Part I, (c) EDX spectrum of coated PIF in Part II, and (d) EDX spectrum of coated PIF in Part III.

Thermal Properties of Uncoated and Silver-Coated PIFs

The thermal stability and pyrolysis products of uncoated and silver-coated PIFs at high temperature were analyzed by a TG-FTIR coupling system. TG and differential thermogravimetric (DTG) curves of uncoated and silver-coated PIFs at a heating rate of 10°C/min in air are shown in Figure 5(a) and (b), respectively. The temperature corresponding to the maximum decomposition temperatures (T_{max}) values can be determined from the DTG curves. The 5% weight loss temperatures ($T_{5\%}$), 10% weight loss temperatures ($T_{10\%}$), residual weight retentions (R_w) at 800°C, and T_{max} of uncoated and coated PIFs are all presented in Figure 5(a, b). As shown in Figure 5(a), the $T_{5\%}$ and $T_{10\%}$ values of uncoated PIF are 300.3°C and 343.4°C, respectively. After being coated with silver, the $T_{5\%}$ and $T_{10\%}$ values increase to about 400.5°C and 440.4°C, respectively. As indicated in Figure 5(b), there are two characteristic temperature regions being observed for both uncoated and coated foams. As for the former, the T_{max} values in region I and region II are 317°C and 543°C, respectively. As for the latter, the T_{max} values in region I and region II are 430°C and 537°C, respectively. We can also see that uncoated PIF degrades faster than coated PIFs in the characteristic temperature region II. The weight loss in region I for both uncoated and silver-coated PIFs can be attributed to the thermal degradation of flexible segments, such as urethane, allophanate, and polyurea, and that in region II for can be due to the thermal pyrolysis of rigid imide structure.¹⁴ It is obviously that PIFs with silver coating exhibit higher thermal stability than uncoated PIF. This increment of

the thermal stability attributed to the thermal stability of silver particles and their enhancing effect. The R_w value of silver-coated PIFs at 800°C are as high as 73.9%; however, the R_w value of uncoated PIF is only 2.8% in air. The pyrolysis residues in silver-coated PIFs in air may be the mixture of the charred coals with high carbon content and silver oxide which generated under high temperature in air.

Absorption strengths of released gases (CO_2 at 2351 cm^{-1} , CO at 2181 cm^{-1} , H_2O at 3745 cm^{-1} , SO_2 at 1099 cm^{-1}) versus

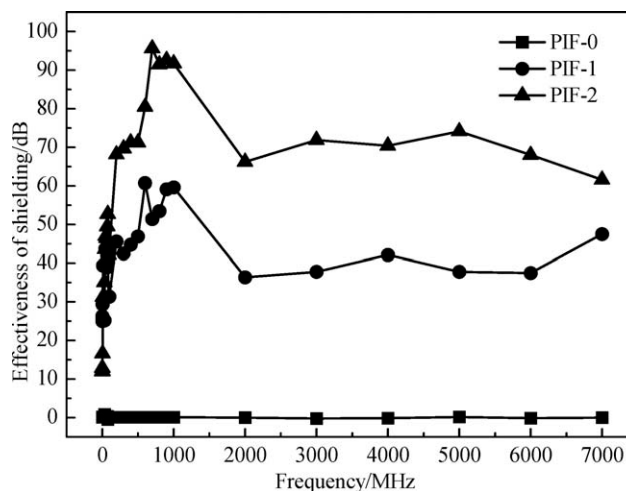


Figure 4. The EMI shielding efficiency of PIF-0, PIF-1, and PIF-2.

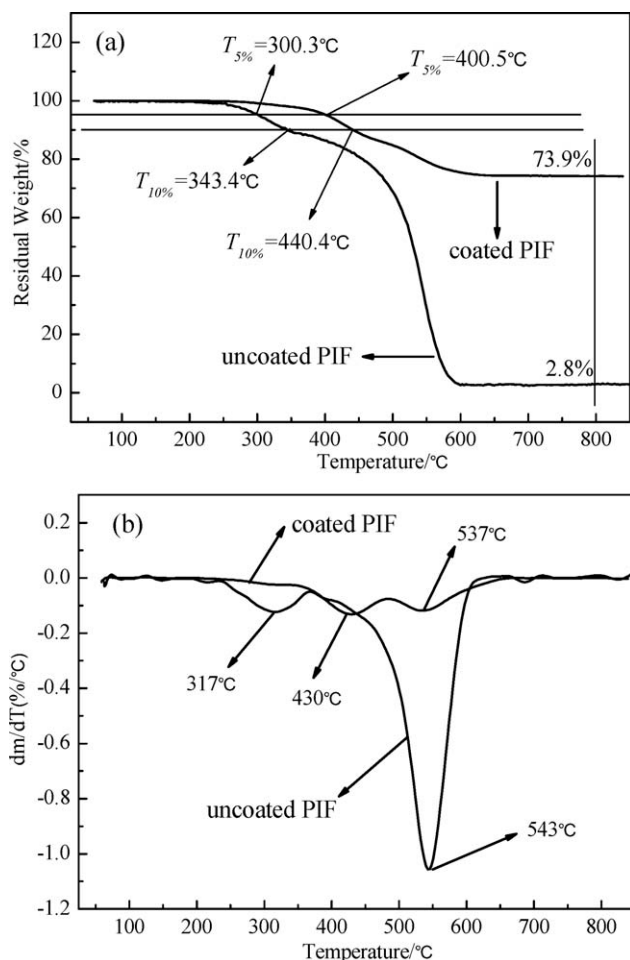


Figure 5. TG and DTG curves of uncoated and silver-coated PIFs.

heating temperature in air for both uncoated and silver-coated PIFs are given in Figure 6(a) and (b), respectively. As illustrated in Figure 6(a), the peaks of the main gaseous decomposition products of uncoated PIF are all located in the temperature range 450–600°C. For silver-coated PIFs, the general peak is located in a wide temperature region from 300 to 600°C. The absorption peak appearing in the temperature range 325–500°C is assigned to the release of SO_2 . Silver sulfide (Ag_2S) is generated when elemental silver is exposed to air, and it is chemically stable at room temperature. However at high temperatures, such as 350°C, the Ag_2S will decompose into SO_2 and Ag. The peaks of CO_2 and H_2O mainly locate in the range of 375–600°C, and the absorption peak of CO disappears in Figure 6(b).

The stacked FTIR spectra of the decomposition products of uncoated and silver-coated PIFs are presented in Figure 7(a) and (b), respectively. The FTIR results show the evolutions of CO_2 , CO, and H_2O derive from uncoated PIF and the evolutions of CO_2 , SO_2 , CO, and H_2O derive from coated PIFs. The characteristic bands of CO_2 are at 2351 cm^{-1} and 690 cm^{-1} . The characteristic band of CO is at 2181 cm^{-1} . The band at 1099 cm^{-1} can be attributed to the stretching vibration of S=O in SO_2 .¹⁴ From Figure 7(a, b) it can be observed that CO_2 exists during the whole decomposition process. At low temperatures, CO_2 may absorb from the atmosphere. At high temperatures, the evolution of CO_2 may be due to the decarboxylation of imide ring and part of them may be also from the atmosphere.

Compressive properties of uncoated and silver-coated PIFs were tested to verify the structural integrity. The typical compression strain–stress curves of these PIFs are shown in Figure 8. The compressive failure of these PIFs goes through three regimes: the first being a linear elastic region, following by a plateau elastic buckling, and finally, a densification region where the cellular

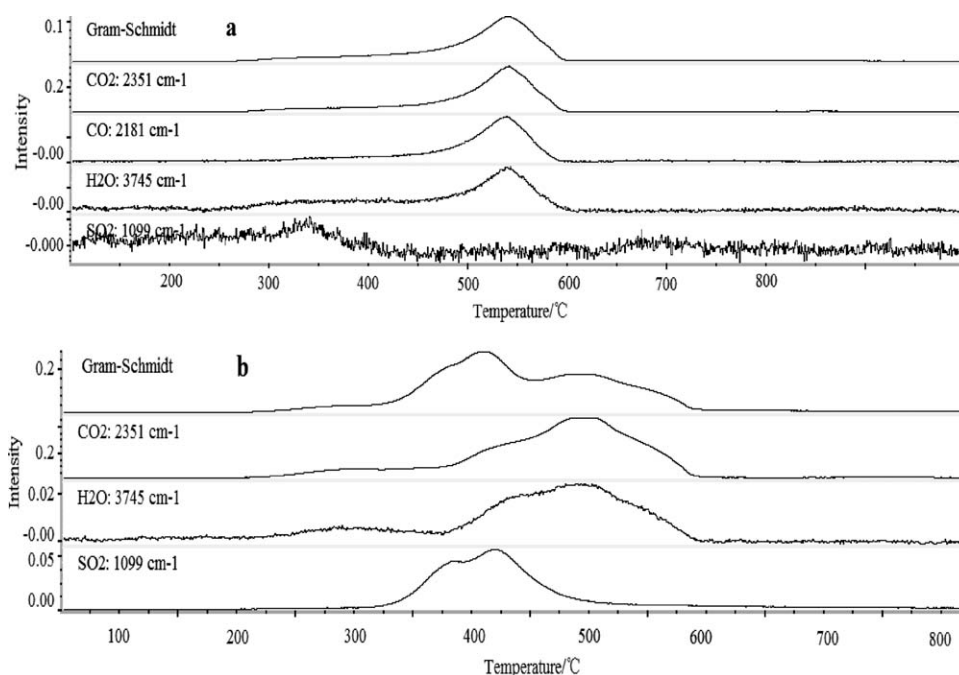


Figure 6. Absorption intensities of PIFs for the by-products measured by FTIR spectra in air: (a) uncoated and (b) silver coated.

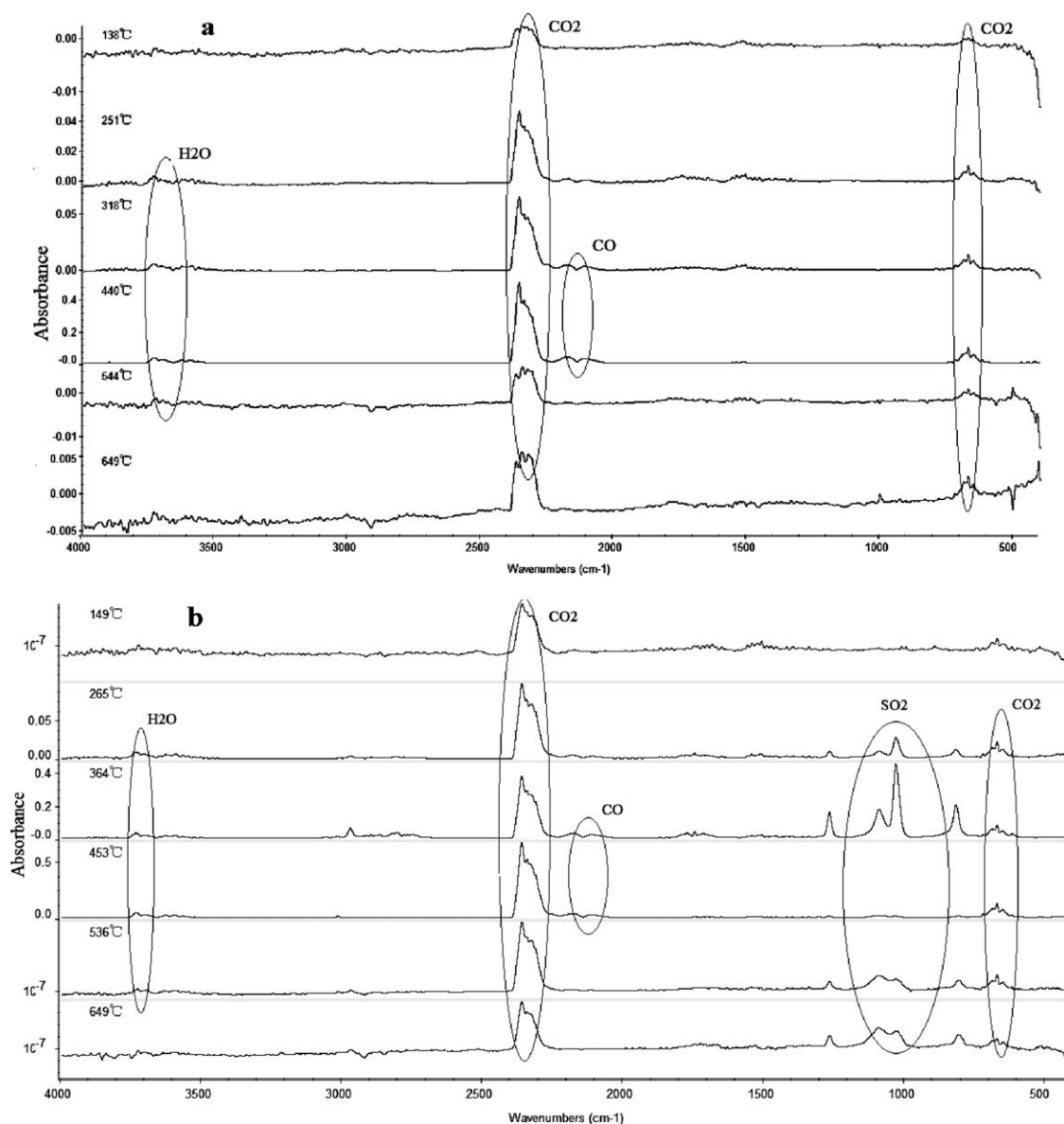


Figure 7. Stacked plot of the FTIR spectra of the gases evolved from PIFs: (a) uncoated and (b) silver coated.

structures are compressed on themselves.¹⁵ As mentioned above, the foam densities of PIF-0, PIF-1, and PIF-2 are 8.3 kg/m³, 15.6 kg/m³, and 22.2 kg/m³, respectively. Therefore, as shown in Figure 8, it is obvious that the compressive strength of PIF-2 is higher than that of PIF-0 and PIF-1, and in the linear elastic region, the compressive strength of PIF-1 is higher than that of PIF-0. Moreover, the silver coatings may play an important role in improve the compressive strength of PIF-2 and PIF-1 in the linear elastic region. The yield strengths of PIF-0, PIF-1, and PIF-2 are 24.1 kPa, 23.7 kPa, and 39.8 kPa, respectively.

CONCLUSIONS

An ultralight and high-temperature resistant EMI shielding polyimide foam was successfully fabricated via a simple and effective strategy. For silver-coated PIFs, the EDX spectrums showed increasing higher silver proportions from interior to exterior sur-

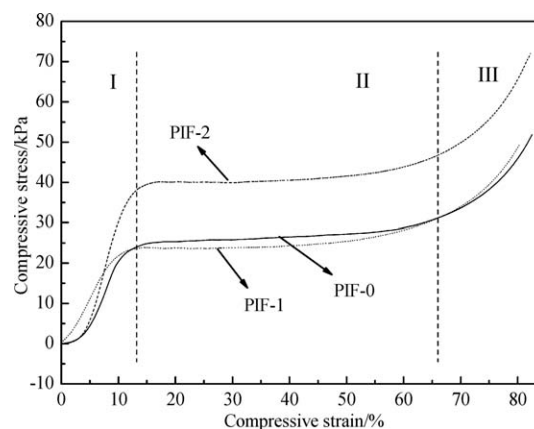


Figure 8. The compressive strain–stress curves of uncoated and silver-coated PIFs.

face, together with increasing higher carbon proportions from exterior surface to interior. The densities of PIF-0, PIF-1, and PIF-2 were not higher than 23 kg/m^3 , which indicate that polyimide foams were ultralight materials. The surface density of silver coating in PIF-1 and PIF-2 was 0.18 kg/m^2 . EMI shielding efficiency provided by PIF-1 at 200–7000 MHz was in the range of 36.4–60.7 dB, with PIF-2 in the range of 61.6–95.6 dB. TG-FTIR results indicated that silver-coated PIFs exhibited excellent thermal stability with 5% weight loss temperatures higher than 400°C because of the high thermal stability of silver particles and their enhancing effect. The compressive strengths scale well with the relative foam densities, especially in the linear elastic region.

ACKNOWLEDGMENTS

This project was sponsored by the National High Technology Research and Development Program of China (863 Program) (No. 2006AA03Z562). Xiao-Yan Liu thank Mao-Sheng Zhan for his help in the guide and the property test.

REFERENCES

1. Chung, D. J. *Mater. Eng. Perform.* **2009**, *9*, 350.
2. Moniruzzaman, M.; Winey, K. I. *Macromolecular* **2006**, *39*, 5194.
3. Li, N.; Huang, Y.; Du, F.; He, X.; Lin, X.; Gao, H. J.; Ma, Y. F.; Li, F. F.; Chen, Y. S.; Eklund, P. C. *Nano. Lett.* **2006**, *6*, 1141.
4. Jing, X. L.; Wang, Y. Y.; Zhang, B. Y. *J. Appl. Polym. Sci.* **2005**, *98*, 2149.
5. Huang, C. Y.; Pai, J. F. J. *J. Appl. Polym. Sci.* **1997**, *63*, 115.
6. Das, N. C.; Chaki, T. K.; Khastgir, D.; Chakraborty, A. J. *Appl. Polym. Sci.* **2001**, *80*, 1601.
7. Wu, G. H.; Huang, X. L.; Dou, Z. Y.; Chen, S.; Jiang, L. T. *J. Mater. Sci.* **2007**, *42*, 2633.
8. Yang, Y.; Gupta, M. C.; Dudley, K. L.; Lawrence, R. W. *Adv. Mater.* **2005**, *17*, 1999.
9. Yang, Y.; Gupta, M. C.; Dudley, K. L.; Lawrence, R. W. *Nano. Lett.* **2005**, *5*, 2131.
10. Zhang, H. B.; Yan, Q.; Zheng, W. G.; He, Z. X.; Yu, Z. Z. *ACS Appl. Mater. Interfaces* **2011**, *3*, 918.
11. Thomassin, J. M.; Pagnouille, C.; Bednarz, L.; Huynen, I.; Jérôme, R.; Detrembleur, C. *J. Mater. Chem.* **2008**, *18*, 792.
12. Xu, X. B.; Li, Z. M.; Shi, L.; Bian, X. C.; Xiang, Z. D. *Small* **2007**, *3*, 408.
13. Liu, X. Y.; Zhan, M. S.; Wang, K.; Li, Y.; Bai, Y. F. *Polym. Adv. Technol.* **2012**, *23*, 677.
14. Shen, Y. X.; Zhan, M. S.; Wang, K.; Li, X. H.; Pan, P. C. *J. Appl. Polym. Sci.* **2010**, *115*, 1680.
15. Williams, M. K.; Weiser, E. S.; Fesmire, J. E.; Grimsley, B. W.; Smith, T. M.; Brenner, J. R.; Nelson, G. L. *Polym. Adv. Technol.* **2005**, *16*, 167.